

Scaling and Topological Charge of a Fixed Point Action for $SU(2)$ Gauge Theory ¹

Thomas DeGrand, Anna Hasenfratz, and Decai Zhu
Department of Physics
University of Colorado, Boulder CO 80309-390

August 2018

Abstract

We construct a few parameter approximate fixed point action for $SU(2)$ pure gauge theory and subject it to scaling tests, via Monte Carlo simulation. We measure the critical coupling for deconfinement for lattices of temporal extent $N_t = 2, 3, 4$, the torelon mass at fixed physical volume, and the string tension (and heavy quark potential) from Wilson loops. We calculate the topological susceptibility using inverse blocking and show that it scales over the observed range of lattice spacings.

¹Work supported in part by NSF Grant PHY-9023257 and U. S. Department of Energy grant DE-FG02-92ER-40672

1 Introduction

In QCD instantons may be responsible for breaking axial symmetry and resolving the $U(1)$ problem [1]. The relevant observable is the topological susceptibility χ , defined as the infinite volume limit of

$$\chi_t = \frac{\langle Q^2 \rangle}{V} \quad (1)$$

where Q is the topological charge and V the space time volume. In QCD χ_t is a dimension-4 object with no weak coupling expansion, and a calculation of χ_t in physical units in the continuum requires nonperturbative techniques. In the large- N_c limit the mass of the η' is related to the topological susceptibility through the Witten-Veneziano formula[2]

$$m_{\eta'}^2 + m_{\eta}^2 - 2m_K^2 = 2N_f \chi_t / f_{\pi}^2. \quad (2)$$

Unfortunately, the study of topology in lattice simulations is badly contaminated by the presence of lattice artifacts, which can arise both from the form of the lattice action and from the choice of lattice operator to define and measure topological charge. A lattice action is, in general, not scale invariant, and so if a smooth continuum instanton is placed on the lattice, its action can depend on its size. A lattice simulation can be compromised by lattice artifacts, called “dislocations,” [3], which are non-zero charged configurations whose contribution to the topological charge comes entirely from small localized regions. If the minimal action of a dislocation is smaller than some critical fraction (6/11 for SU(2)) of the continuum value of a one-instanton configuration, then dislocations will dominate the path integral and spoil the scaling of χ_t [4, 5]. Difficulties also arise because the topological charge is not conserved on the lattice. When the size of an instanton becomes small compared to the lattice spacing it can “fall through” the lattice and its charge disappears. Topological charge operators can fail to identify this process.

In Ref. [6] we described a framework which solves both these problems and allows one to study topology in the context of numerical lattice simulations in a theoretically reliable way. If one can construct a lattice action and lattice operators which live on the renormalized trajectory (RT) of some renormalization group transformation (RGT), then one’s predictions do not depend on the lattice spacing. A recent series of papers[7, 8, 9, 10] have constructed fixed point (FP) actions for asymptotically free spin and gauge theories. FP actions share the scaling properties of the RT (through one-loop quantum corrections) and as such may be taken as a first approximation to a RT. FP gauge actions have scale-invariant instanton solutions with an action value of exactly $8\pi^2/g^2$ and, using

RG techniques, one can define a topological charge which has no lattice artifacts. Basically, one inverts an RG transformation using a FP action to produce a fine-grained lattice which has the same topological structure as the original coarse configuration. On the fine lattice the size of any topological object scales as the ratio of coarse to fine lattice spacings, and after enough blocking steps the objects will become so large that their charge can be measured in any way desired.

The purpose of this paper is to construct an approximate FP action for SU(2) pure gauge theory, subject it to scaling tests, and then measure the topological susceptibility. In the next section we outline the construction of an action. Then we describe its properties under simulation: we have computed the critical temperatures for deconfinement, and the string tension measured using correlators of Polyakov loops and from Wilson loops. The action shows good scaling properties beginning at lattice spacing $a \leq 1/2T_c$. Finally we describe our measurement of the topological susceptibility using inverse blocking.

We (again) remark that our approach to topology has been anticipated by studies by others of two-dimensional spin models[11, 12, 13], although we cannot go as far due to computer speed and memory limitations.

2 Construction of an Approximate FP Action

In order to have a practical action for use in simulations, we adopt a slightly different method for finding a FP action than was used in Ref. [6]. We want an action valid only for configurations which would be encountered in a realistic simulation, with correlation lengths of a few lattice spacings. Thus we solve the FP steepest descent equation

$$S^{FP}(V) = \min_{\{U\}} (S^{FP}(U) + T(U, V)), \quad (3)$$

(where $\{V\}$ is the coarse configuration, $\{U\}$ is the fine configuration, and $T(U, V)$ is the blocking transformation) as follows: we generate coarse configurations using the Wilson action with Wilson coupling $\beta = 1.5 - 2.5$ and perform the minimization to find the number $S^{FP}(V)$. We use an algorithm similar to the one we employed for SU(3) gauge theory [9], making a random rotation on each link variable and quadratically interpolating to a proposed minimum. The cost of a sweep through the lattice is roughly equivalent to a standard Monte Carlo update sweep. We reduced the change in the action per sweep to a value of 0.005 or below. Typical action values range from 1000 to 8000, depending on the volume of the lattice and the coupling. The number of sweeps required

to minimize the configuration to the given accuracy is strongly beta-dependent, the procedure gets increasingly costly at small β values.

We fit $S^{FP}(V)$ measured according to Eqn. 3 to a small set of operators and couplings. The fit is not designed to work for configurations which are much smoother or coarser than the ones we present to be minimized. There is considerable freedom in this fitting method, and it may be that alternate approximate FP actions exist which solve Eqn. 3 equally well, and have other nicer properties in addition.

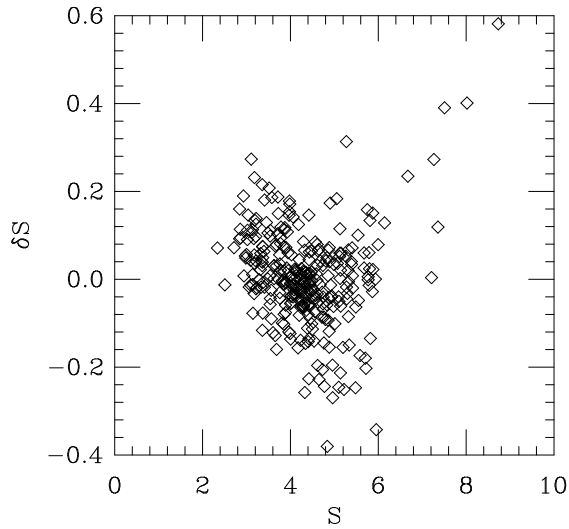


Figure 1: Difference between the measured (Eqn. 3) and fitted (Eqn. 4) value of $S_{FP}(V)$ for the eight parameter approximate FP action of Table 1.

The approximate FP action consists of several powers of two loops, the

plaquette and the perimeter-six loop (x,y,z,-x,-y,-z),

$$S(V) = \frac{1}{2} \sum_C (c_1(C)(2 - \text{Tr}(V_C)) + c_2(C)(2 - \text{Tr}(V_C))^2 + \dots) \quad (4)$$

with coefficients tabulated in Table 1. The quality of the fit is shown in the scatter plot of Fig. 1. We chose the c_1 coefficients so that the approximate FP action is $O(a^2)$ improved.

Table 1: Couplings of the few-parameter FP action for SU(2) pure gauge theory.

operator	c_1	c_2	c_3	c_4
c_{plaq}	.3333	.00402	.00674	.0152
c_{6-link}	.08333	.0156	.0149	-.0035

In Ref. [6] we constructed sets of trial smooth instantons and measured their action and charge. We found that when they had $Q = 1$, their action $S(\rho) \geq S_I$, where S_I is the continuum instanton action, and that dislocations (instanton-like field configurations for which $Q \neq 1$) have actions evaluated at the FP using inverse blocking which is less than S_I . Now we make a similar comparison for these configurations using our approximate FP action. We consider two kinds of smooth configurations, singly blocked c_1 and c_2 instantons (for a description of these objects see Ref. [6].) We show actions versus instanton size ρ in Figs. 2 and 3. The dotted line indicates the $Q = 0 \rightarrow Q = 1$ boundary on the original coarse lattice while the solid line is the boundary on the inverse blocked configuration. Instanton configurations were not included in the fit which produced the action. The curve shows the action on the coarse lattice evaluated according to Eqn. 3 and Table 1. The action does not reproduce the good feature of the full FP action: in particular, $S(\rho) < S_I$ out to very large ρ . However, this action is still quite suitable for simulations. It will generate dislocations (configurations which have $Q = 1$ but $S < S_I$), but those dislocations will not dominate the functional integral because their action exceeds the entropic bound (for SU(N)) of

$$S > \frac{48\pi^2}{11N^2}, \quad (5)$$

or $S/S_I > 6/11$ for $SU(2)$. If we measure the action on an inverse blocked lattice using a parameterization of the FP action appropriate to smooth gauge configurations we will reproduce the results of Ref. [6], namely $S(\rho) \geq S_I$ when $Q = 1$, $Q = 0$ when $S(\rho) < S_I$.

3 Critical Couplings for Deconfinement

The deconfinement phase transition for the pure SU(2) gauge theory is second order, and the transition is in the same universality class as the three-dimensional Ising model. The order parameter is the average Polyakov loop

$$L = \frac{1}{N_s^3} \sum_{\vec{x}} L(\vec{x}) \quad (6)$$

where

$$L(\vec{x}) = \frac{1}{2} \text{Tr} \prod_{t=1}^{t=N_t} U_{t,\vec{x};0} \quad (7)$$

and N_s and N_t are the spatial and temporal size of the lattice respectively.

The Binder cumulant is defined as

$$g_4 = \frac{\langle L^4 \rangle}{\langle L^2 \rangle^2} - 3. \quad (8)$$

A standard finite size scaling analysis shows that this quantity is a scaling function [14]. It must be independent of N_s at the critical point (neglecting contributions from irrelevant scaling fields).

In order to determine the critical coupling, we run simulations at different N_s for each N_t , then plot the Binder cumulant. The location in β at which the different curves cross must correspond to the critical point.

Fig. 4 shows the Binder cumulant plot for $N_t = 2$. We performed simulations at three different volumes, $N_s = 4, 6$ and 8 . From this plot, we see that the crossing happens at approximately $\beta = 1.34$ and $g_4 = -1.40$, which is consistent with the result from the three-dimensional Ising model where $g_4 = -1.41(1)$ [15]. Combining this plot and the requirement that $g_4 = -1.40$ at the crossing, we conclude that $\beta_c = 1.340(5)$ for $N_t = 2$.

Figs. 5 and 6 show the Binder cumulant plots for $N_t = 3$ and $N_t = 4$. It is difficult to decrease the statistical error for these data points. We identify the critical coupling as the point where $g_4 = -1.40$, and so we conclude that $\beta_c = 1.502(5)$ and $1.575(10)$ for $N_t = 3$ and 4 , respectively.

Although the FP action is not designed to improve asymptotic scaling, only scaling, we can still see if it shows asymptotic scaling. Using the original coupling in the action, we compute T_c/Λ from the two loop formula from our data,

and record the results in Table 2 and Fig. 7. The eight parameter FP action shows asymptotic scaling within fifteen per cent from $N_T = 2$ to 4 in terms of the bare coupling, with $T_c/\Lambda \simeq 7 - 8$. Its Λ parameter is about a factor of five larger than the Wilson one and therefore much closer in value to the continuum Λ parameters.

Table 2: Critical couplings at infinite volume for the FP action with parameters in Table 1.

N_t	2	3	4
β_c	1.340(5)	1.502(5)	1.575(10)
T_c/Λ	8.01(9)	7.87(9)	7.04(17)

4 Torelon Mass

In this section we describe the measurement of the string tension σ through the correlator of pairs of objects with the quantum numbers of Polyakov loops: on a lattice of transverse size L the correlator of two Polyakov loops averaged over transverse separations and separated a longitudinal distance z is

$$C(z) = \sum_{r_\perp} \text{Re} \langle P_j(r_\perp, z) P_j^\dagger(0, 0) \rangle \simeq \exp(-\mu z) \quad (9)$$

(plus boundary terms) where μ is the so-called torelon mass. On an infinite lattice $\mu = \sigma L$ and we will define $\mu = L\sigma(L)$ on a finite lattice. To carry out a scaling test we fix the lattice spacing through the deconfinement temperature and perform a series of simulations on lattices of fixed physical size $L = c/T_c$ and different lattice spacings. Here we take $c = 2$ and $aT_c = 1/2, 1/3$, and $1/4$ (the corresponding couplings were determined in the previous section). As a scaling test we compute $L\sqrt{\sigma} = c\sqrt{\sigma}/T_c$.

At large lattice spacing ($aT_c = 1/2$) the best signals came from the Polyakov loop itself, measured with the Parisi - Petronzio - Rapuano [16] multihit variance reduction method. At smaller lattice spacing ($aT_c \leq 1/3$) we used correlators of APE-blocked [17] links: we iterate

$$V_j^{n+1}(x) = (1 - \alpha)V_j^n(x) + \alpha/4 \sum_{k \neq j} (V_k^n(x)V_j^n(x + \hat{k})V_j^n(x + \hat{j})^\dagger + V_k^n(x - \hat{k})^\dagger V_j^n(x - \hat{k})V_j^n(x - \hat{k} + \hat{j})) \quad (10)$$

(with $V_j^0(x) = U_j(x)$ and $V_j^{n+1}(x)$ projected back onto $SU(2)$), with α varying from 0.2 at $aT_c = 1/3$ to 0.5 at $aT_c = 1/4$ and ten blocking steps.

We determined the torelon mass from a single-exponential correlated fit, beginning at a minimum z where the χ^2/DF is near unity, and where we see stability in the effective mass over a range of z . At $aT_c = 1/2$ the fits are to $z = 1$ and $z = 2$ points only since there is no signal for $z > 2$.

We display our results in Fig. 8 and Tables 3 and 4. An uncertainty in the value of the critical coupling propagates into the uncertainty of $L\sqrt{\sigma(L)} = 2\sqrt{\sigma}/T_c$ for the FP action. We include this uncertainty in the figure by combining it in quadrature with the statistical fluctuation in $L\sqrt{\sigma(L)}$; in the figure the extreme range of the vertical error bars shows the combined uncertainty.

Table 3: Our measurements of torelon masses from the Wilson action on small lattices.

volume	β	$\mu = L\sigma$	$L\sqrt{\sigma}$
$4^3 \times 12$	1.88	2.25(5)	3.00(3)
$6^3 \times 12$	2.177	1.38(3)	2.88(3)
$8^3 \times 12$	2.29872	0.97(3)	2.78(4)

Table 4: Our measurements of torelon masses from the FP action.

volume	β	$\mu = L\sigma$	$L\sqrt{\sigma}$
$4^3 \times 12$	1.34	1.75(6)	2.65(4)
$6^3 \times 12$	1.502	1.16(7)	2.62(2)
$8^3 \times 12$	1.575	0.82(3)	2.55(4)

There have been many simulations in the literature which present the string tension from the torelon mass [18, 19, 20]. However, most of them are done on lattices whose physical size is not the one used here, $L = 2/T_c$. On the scale of Fig. 8 the torelon mass $\sigma(L)$ is quite sensitive to L . We elect to show only three small lattice spacing points. The first is the Wilson action $\beta = 2.50$ 16^4 result of Michael and Teper[18]; for this data set, $L \simeq 2.07/T_c$ (a lattice with $N_t = 7.7$ would be at its deconfinement transition at $\beta = 2.50$). We also show the $\beta = 2.60$ point of the same authors and the $\beta = 2.70$ point of Ref. [19]; for these data we extrapolate to $L = 2/T_c$ using the string formula

$$\sigma = \sigma(L) + \frac{\pi}{3L^2} \quad (11)$$

(which itself may not be correct).

The result of our simulations is that the torelon mass measured on aspect ratio 2 lattices using the FP action scales within one standard deviation for $1/4 \leq aT_c \leq 1/2$, at a value which appears to be consistent with the value inferred from Wilson action results from small lattice spacing simulations.

5 Potential from Wilson Loops

As β rises, the critical temperature for deconfinement becomes more difficult to measure, and one needs some other quantity to determine the scale. Torelons are not a good choice because of their sensitivity to volume. The only other relatively straightforward observable is the potential, extracted from $L \times T$ Wilson loops $W(L, T)$.

We used a method (and a program) developed by U. Heller[21]: we construct APE-blocked spatial links and measure Wilson loops made of these blocked spatial links and unblocked temporal links. This gives a better overlap onto the potential. To speed up the program, the computation of the Wilson loops is done by first performing a gauge transformation to axial gauge, after which the desired APE smearing of space-like links is accomplished. We measure all on-axis loops, as well as off-axis time-like loops with the space-like parts along the directions $(1,1,0)$, $(2,1,0)$ and $(1,1,1)$ plus others related by the lattice symmetry.

The potential is defined up to an additive constant by

$$\exp(-V(R)T) = W(R, T) \quad (12)$$

and is measured by fitting the analog of the “effective mass” in spectroscopy: look at the ratio $-\log(W(R, T+1)/W(R, T))$ and ask for it to plateau; then equate it to the potential $V(R)$.

These are low-statistics simulations. We used a $12^3 \times 16$ lattice (8^4 for Wilson $\beta = 1.88$, FP $\beta \leq 1.45$) and collected 100-500 measurements of Wilson loops (spaced five update sweeps apart) per coupling.

While the numerics are easy the analysis is not. The signal from big R disappears into the noise exponentially in R (as the torelon mass does) and the extraction of $V(R)$ from the data requires a global fit to some functional form. However, as far as we can tell, the choice of a particular ansatz is arbitrary. It is difficult to make reliable error estimates if the results depend on it.

In Table 5 we present the result of a fit to $V(r)$ to the form

$$V(r) = V_0 + \sigma r - E/r - F(G_L(r) - 1/r) \quad (13)$$

with $G_L(r)$ the lattice Coulomb potential for the quadratic action (i.e. the action given by truncating the formula of Table 1 by keeping only the c_1 terms, then expanding $2 - \text{Tr}U$ to quadratic order in the vector potential). A fit to the form

$$V(r) = V_0 + \sigma r - E/r \quad (14)$$

produces essentially identical results for σ for the smaller lattice spacing data ($\beta > 1.502$). The larger lattice spacing data are difficult to fit. The FP $\beta = 1.34$ data set is fit keeping only on-axis points, and is fit to pure linear plus Coulomb form. The Wilson $\beta = 1.88$ data is fit keeping only the linear term.

A scale related to the string tension, which has smaller dependence on the functional form of $V(r)$, is the distance r_0 , as defined through the force, by $r_0^2 F(r_0) = -1.65$ [22]. In the physical world of three colors and four flavors, $r_0 = 0.5$ fm. The last column of Table 5 shows r_0 for our data.

Table 5: Parameters of the static potential from Wilson loops.

FP action					
β	$a^2\sigma$	χ^2	r_{min}	r_{max}	r_0/a
1.7	0.051(1)	12.5	1.00	7.07	5.10(15)
1.65	0.082(1)	6.7	1.41	6.93	4.15(10)
1.625	0.093(2)	8.1	2.00	8.49	3.9(1)
1.6	0.111(2)	17.138	1.73	8.66	3.55(10)
1.575	0.133(2)	14.5	1.73	10.3	3.25(10)
1.502	0.237(7)	14.5	2.24	8.49	2.48(5)
1.45	0.35(1)	5.6	2.24	5.56	2.05(10)
1.34	0.51(2)	1.0	1.00	4.00	1.7(1)
Wilson action					
2.2987	.142(2)	3.2	2.24	5.2	3.1(1)
1.88	0.67(2)	.07	2	4	1.6(1)

The $\beta = 1.34, 1.502$, and 1.575 points can be used for a second scaling test since they are at $aT_c = 1/2, 1/3$ and $1/4$: $\sqrt{\sigma}/T_c = 1.43(3), 1.46(2)$, and $1.46(1)$. (The errors do not include an uncertainty in β_c).

In contrast the Wilson action string tension shows an eight per cent violation of scaling between $N_t = 2$ and 4 , with $\sqrt{\sigma}/T_c$ at $N_t = 2$ of $1.63(3)$ and at $N_t = 4$ of $1.51(1)$.

Because we only use naive operators for the potential, not FP operators[8], the presence or absence of rotational symmetry breaking is not a scaling test. The persistence of such violation as the lattice spacing changes is a test of scale breaking. We can compare violations of rotational symmetry as a function of lattice spacing by using our results from lattice spacings determined from T_c , by scaling the potential by $1/T_c$ and the radius by T_c . We display the scaled potentials from the Wilson action in Fig. 9 and from the FP action in Fig. 10. We have not forced the potentials to lie atop each other, so the reader can view the extent of rotational symmetry violations.

The combination $r_0^2\sigma$ is a dimensionless variable whose variation with lattice spacing gives a scaling test (to the extent that the determination of r_0 and/or σ can be compromised by lack of rotational invariance). We present a plot of $r_0^2\sigma$ vs a/r_0 (lattice spacing in units of 0.5 fm) in Fig. 11. The dominant uncertainty is from the string tension. Both Wilson and FP actions scale within our uncertainties for this variable.

6 Topological Susceptibility

In Ref. [6] we described how to use the scale invariance of the FP action to define topological charge through an RG transformation by interpolating the gauge field configuration generated on a coarse lattice to a finer lattice. The interpolation is done by solving Eqn. 3. We then measure the instanton charge on the fine lattice. If the configurations are generated using a FP action and inverse blocked using the same FP action, the blocking preserves the topological charge while doubling the radius of any instanton. In principle this procedure should be repeated until all of the instantons generated on the coarse lattice have inflated to such a large size that any measuring technique will give their charge. In practice, we are limited to a single step of inverse blocking, which might not prove reliable if the initial configuration is too rough.

We measure the topological charge in the following way: We generate a series of gauge configurations $\{V\}$ on an L^4 lattice using the eight-parameter approximate FP action of Table 1. We then inverse block the configurations onto a $(2L)^4$ lattice to produce fine variables $\{U\}$, by solving Eqn. 3. Finally, we define the topological charge on the configuration as its value on the fine lattice, measured using the geometric definition [23]

$$Q(V) = Q_{geom}(U). \tag{15}$$

We use the same minimizing algorithm as we used for the construction of the action in Section 2. Inverse blocking is carried out on the fine lattice and typically takes 50 to 200 minimization passes through the lattice. We reduced the change in the action per sweep to a value of 0.001 or below, while typical action values range from 1000 to 8000. For most configurations this accuracy is not necessary, but occasionally the topological charge will change as we reduce the change in the action from, for example, 0.01 to 0.001. For the topological susceptibility we have not observed any systematic difference, though.

To perform a scaling test we compute the dimensionless ratio of susceptibility

times the fourth power of r_0

$$\chi r_0^4 = \langle Q^2 \rangle \left(\frac{r_0}{L}\right)^4 \quad (16)$$

where r_0 is extracted from the heavy quark potential. An alternative would be the ratio of susceptibility divided by the square of the string tension

$$\frac{\chi}{\sigma^2} = \frac{\langle Q^2 \rangle}{L^4 \sigma^2} \quad (17)$$

but r_0 has a smaller overall systematic uncertainty with respect to form of the potential and fit range.

In measuring the topological charge one encounters two types of systematic errors even when the action itself shows scaling. The first is the effect of finite volume: on small volumes larger instantons are lost and the measured susceptibility is smaller than on infinite volume. The second effect is related to finite lattice spacing: small radius instantons are not supported on lattices with large lattice spacing, again lowering the measured value of the topological susceptibility. In the following we compare the scale invariant quantity χr_0^4 on lattices of fixed physical size, measured in units of r_0 but of different lattice spacing (again measured in units of r_0).

Table 6 contains our measurements for the topological susceptibility for the approximate fixed point action. The data sets typically contain 300-400 independent configurations. For comparison we also present $\langle Q^2 \rangle$ measured directly on the coarse lattice (no inverse blocking). This number is about a factor of 3-4 larger than the theoretically reliable inverse blocked number, signaling that small dislocations on the coarse lattice have been incorrectly identified as instantons by the geometric algorithm.

For the Wilson action the topological susceptibility has been measured both by the direct geometric definition and after cooling (locally minimizing the action) [24]. Typically, the charge on cooled configurations was found to be about 1/10 the charge measured on coarse configurations. Cooling has been regarded with misgiving by some authors, because of fear that some objects carrying topological charge would disappear under cooling. Our results indicate that those fears were justified. It may still be possible to find a cooling algorithm which reproduces the results of inverse blocking, but we feel that it would have to be used with extreme caution. We were not able to invent a satisfactory cooling method.

All the results for $\langle Q^2 \rangle_{min}$ of Table 6 have been obtained after one inverse blocking step. We performed a short test run at $\beta = 1.6$ where we inverse

blocked twice, from 4^4 to 8^4 to 16^4 lattices. On all configurations the topological charge was identical after one and two inverse blocking steps.

In Figure 12 we plot the quantity χr_0^4 versus the lattice spacing a/r_0 for physical volumes $L/r_0 \sim 1.6, 1.9$ and 3.2 . The three data points corresponding to $L/r_0 = 1.54, 1.57$ and 1.62 , which span a range in lattice spacing $a = 0.4r_0 - 0.2r_0$ is consistent with scaling. Apparently a lattice with $a = 0.4r_0$ is fine enough to support the physically relevant instantons. To check that assumption further, we created a set of 4^4 configurations by blocking with the RG transformation of the FP a set of 8^4 configurations generated at $\beta = 1.7$. The scaling properties and the value of L/r_0 of these configurations are the same as the 8^4 configurations but the lattice spacing is doubled by the blocking. Any change in the topological susceptibility would be due to the large lattice spacing $a = 0.4r_0$ of the 4^4 configurations. The blocked lattices are much rougher than the original ones, and the signal is noisier. It is likely that more than one inverse blocking step is needed to smooth the configuration. However, within our accuracy no difference is seen in the topological susceptibility.

In contrast the topological susceptibility on the coarsest lattice $a = 0.5r_0$ of the volume $L/r_0 = 1.85, 1.93$ and 1.95 set is a bit lower than the two finer lattice values. This lattice is too coarse for the relevant instantons. In physical units, a lattice spacing of 0.25 fm is coarse enough to affect the topological properties of QCD while a spacing of 0.2 fm seems to be small enough not to do so. According to our earlier work [6], a candidate instanton solution has $Q = 1$ only if $\rho/a > 0.7 - 0.8$: thus physically relevant instantons have sizes larger than $0.2 \times (0.7 - 0.8)$ fm or about 0.16 fm.

Within our statistical errors there is no significant change in the topological susceptibility as we increase the volume of the lattice.

Making the (possibly unwarranted) assumption that the large volume is large enough to approximate infinity, and making the (also possibly unwarranted) assumption that the pure gauge $SU(2)$ r_0 is equal to the phenomenological $SU(3)$ number 0.5 fm, our value $\chi r_0^4 = 0.12(2)$ corresponds to $\chi = (235(10) \text{ MeV})^4$. Evaluating the Witten-Veneziano formula with the known physical masses of the appropriate mesons, and $N_f = 3$, this susceptibility yields an η' mass of 1520 MeV. With the physical η' mass, one would expect to see $\xi^{1/4} = 180$ MeV if all the assumptions which went into the derivation of Eqn. 2 were correct.

Table 6: Topological charge from the approximate FP action.

β	L	Q^2 direct	Q^2 min	L/r_0	χr_0^4
1.45	4	2.79(38)	1.020(100)	1.95	0.070(21)
1.502	4	2.01(8)	.540(026)	1.62	0.079(10)
1.502	6	9.8(8)	3.15(29)	2.42	0.091(16)
1.502	8	37.5(43)	11.55(87)	3.23	0.106(17)
1.575	6	3.96(27)	1.463(116)	1.85	0.126(25)
1.6	6	2.92(12)	.727(078)	1.69	0.089(19)
1.6	8	10.2(8)	3.13(33)	2.25	0.0140(29)
1.625	6	1.98(10)	.490(029)	1.54	0.087(14)
1.65	8	5.18(34)	1.520(105)	1.93	0.110(18)
1.7	8	2.21(11)	.503(030)	1.57	0.083(15)
1.7	8 \rightarrow 4		.60(6)	1.57	0.099(21)

7 Conclusions

We demonstrate that an FP action shows scaling in the ratio σ/T_c , where the string tension is computed from the torelon mass, as opposed to the Wilson action, where the scaling violations are about eight per cent for the same range of lattice spacings.

We measured the topological susceptibility of SU(2) pure gauge theory using a theoretically motivated technique. We found the topological susceptibility on lattices with $L/r_0 \leq 1.6$, $a \leq 0.4r_0$ is $\chi r_0^4 = 0.12(2)$. In physical units that corresponds to $\chi^{1/4} = 235$ MeV.

The major bottleneck in the computation is, of course, the inverse blocking. The inverse block transformation creates a smooth lattice from a coarse one. In this sense it is an interpolating transformation like that of Ref. [25]. However topological properties are not necessarily preserved by all interpolating transformations. In our case Eqn. 3 guarantees that the topological charge is the same on the coarse lattice and on the interpolating fine lattice. It may be that one can devise an approximate parametrization of the inverse blocked lattice along the lines of the construction for the sigma model described in Ref. [11], or that the procedure of Ref. [25] could be refined for the given RG transformation. It is also possible that the construction of Ref. [25] could be used as a starting point for further numerical minimization.

The extension of all these methods to SU(3) appears to be straightforward. We encourage others interested in the topological properties of gauge theories to use them. We remind the reader one last time that the essential ingredient of

our technique is the use of a FP action and of an interpolation (inverse blocking) which exploits the scaling properties of the FP action, to transform lattice configurations which are so rough that standard measurements of topological charge fail, into smoother configurations which still retain all the original topological properties. On these configurations the charge can be reliably measured. The method has to be used with a FP action. Generating configurations with the Wilson action and inverse blocking them with our RG kernel is not consistent.

8 Acknowledgements

We would like to thank M. Müller-Preussker for providing us with a copy of the program for measuring topological charge. We very much want to thank Urs Heller for his analysis of the potential using Wilson loops, described in Section 5. We would like to thank P. Hasenfratz and F. Niedermayer for useful conversations, and A. Barker, M. Horanyi and the Colorado high energy experimental group for allowing us to use their work stations. This work was supported by the U.S. Department of Energy and by the National Science Foundation.

References

- [1] S. Weinberg, Phys. Rev. D11 (1975) 3583; G. t'Hooft, Phys. Rev. D14 (1976) 3432; Phys. Rev. Lett. 37 (1976) 8.
- [2] E. Witten, Nucl. Phys. B156 (1979) 269; G. Veneziano, Nucl. Phys. B159 (1979) 213.
- [3] M. Kremer, A. S. Kronfeld, M. L. Laursen, G. Schierholz, C. Schleiermacher and U.-J. Wiese, Nucl. Phys. B305 (1988) 109.
- [4] D. J. R. Pugh and M. Teper, Phys. Lett. 224B (1989) 159.
- [5] M. Göckeler, A. S. Kronfeld, M. L. Laursen, G. Schierholz, and U.-J. Wiese, Phys. Lett. 233B (1989) 192.
- [6] T. DeGrand, A. Hasenfratz, D. Zhu, COLO-HEP-369, hep-lat/9603015.
- [7] P. Hasenfratz and F. Niedermayer, Nucl. Phys. B414 (1994) 785; P. Hasenfratz, Nucl. Phys. B (Proc. Suppl) 34 (1994) 3; F. Niedermayer, *ibid.*, 513.
- [8] T. DeGrand, A. Hasenfratz, P. Hasenfratz, F. Niedermayer, Nucl. Phys. **B454** (1995) 587.

- [9] T. DeGrand, A. Hasenfratz, P. Hasenfratz, F. Niedermayer, Nucl. Phys. **B454** (1995) 615.
- [10] A. Farchioni, P. Hasenfratz, F. Niedermayer and A. Papa, BUTP-95/16, IFUP-TH 33/95, preprint (1995).
- [11] M. Blatter, R. Burkhalter, P. Hasenfratz and F. Niedermayer, Nucl. Phys. **B** (Proc. Suppl.) 42 (1995) 799; Bern preprint BUTP 95/17, hep-lat/9508028.
- [12] R. Burkhalter, Bern preprint BUTP-95/18, hep-lat/9512032.
- [13] M. D'Elia, F. Farchioni, A. Papa, Bern preprint IFUP-TH 60/95 (1995): hep-lat/9511021.
- [14] J. Engels, J. Fingberg and M. Weber, Nucl. Phys. **B332**(1990) 737.
- [15] A.M. Ferrenberg and D.P. Landau, Phys. Rev. **B44**(1991) 5081; V. Privman, P. Hohenberg and A. Aharony, *in* phase transitions and critical phenomena, Vol. 14, ed. C. Domb and J. Lebowitz (Academic Press, New York, 1991).
- [16] G. Parisi, R. Petronzio, F. Rapuano, Phys. Lett. **128B**, 418 (1983).
- [17] M. Falcioni, M. Paciello, G. Parisi, B. Taglienti, Nucl. Phys. **B251**[FS13], 624 (1985). M. Albanese, et. al. Phys. Lett. **B192**, 163 (1987).
- [18] C. Michael and M. Teper, Nucl. Phys. **B305** [FS23] (1988) 453.
- [19] C. Michael and S. Perantonis, in the Proceedings of Lattice '90, Nucl. Phys. **B** [Proc. Suppl.] 20, (1991) 177.
- [20] S. Booth, et. al., Nucl. Phys. **B394** (1993) 509.
- [21] U. Heller, K. Bitar, R. Edwards, A. Kennedy, Phys. Lett. **335B**, 71 (1994).
- [22] R. Sommer, Nucl. Phys. **B411** (1994) 839.
- [23] M. Luscher, Commun. Math. Phys. **85** (1982) 29; A. Phillips and D. Stone, Commun. Math. Phys. **103** (1986) 599.
- [24] D. J. R. Pugh, M. Teper, Phys. Rev. Lett. **B218** (1989), 326.
- [25] P. Hernández and R. Sundrum, Harvard preprints HUTP-96/A015, hep-lat/9604009 and HUTP-96/A003, hep-lat/9602017 (1996).

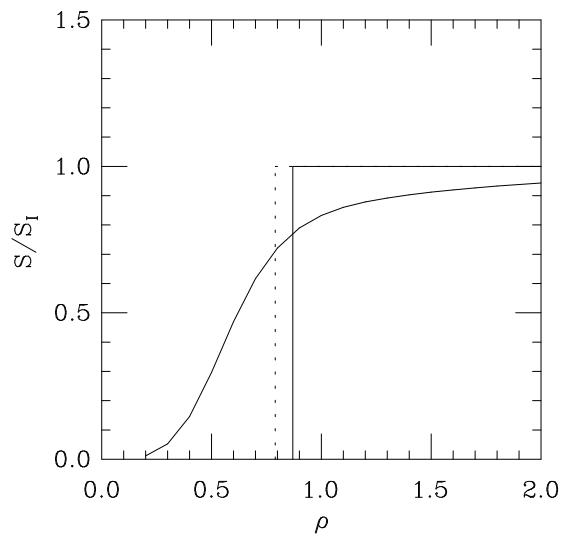


Figure 2: Action of single blocked c_1 instanton configurations computed using the eight parameter FP action. The dotted line indicates the $Q = 0 \rightarrow Q = 1$ boundary on the original coarse lattice while the solid line is the boundary on the inverse blocked configuration.

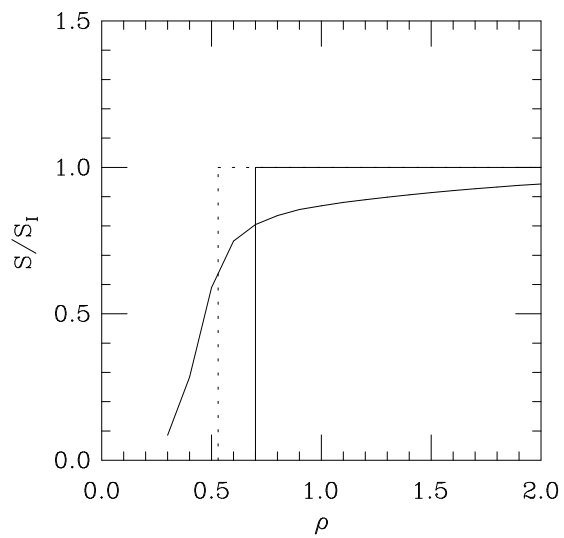


Figure 3: Action of single blocked c_2 instanton configurations computed using the eight parameter FP action, displayed as in Fig. 2.

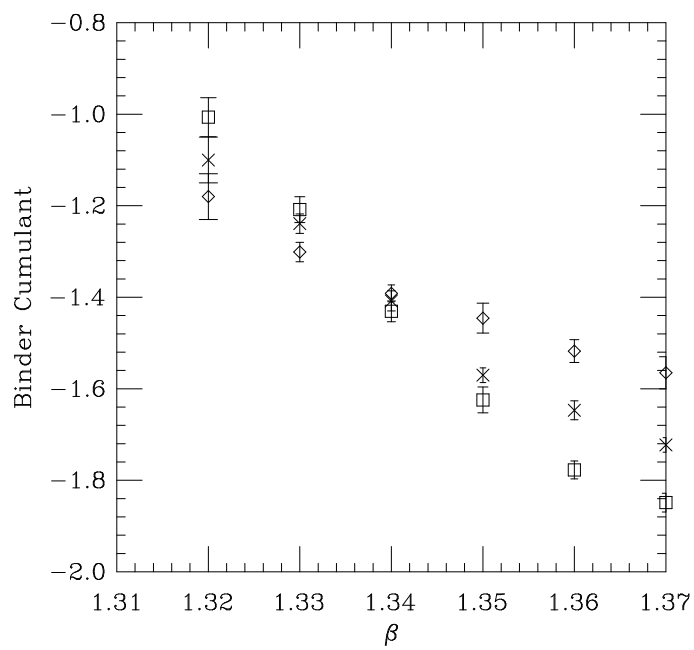


Figure 4: The Binder cumulant for the FP action for $N_t = 2$. The diamond shows results for 4^3 spatial volumes, the cross labels 6^3 volumes, and the square labels 8^3 .

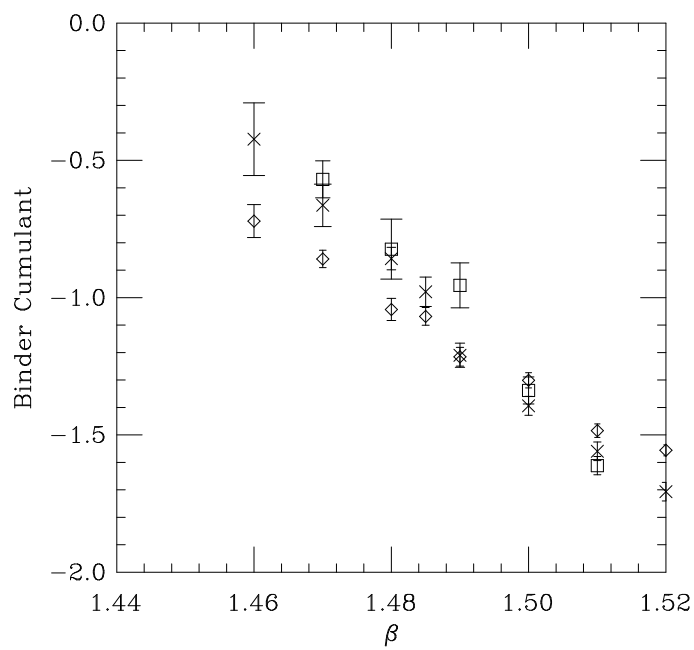


Figure 5: The Binder cumulant for the FP action for $N_t = 3$. Diamond: 6^4 , cross: 8^3 and square: 10^3 spatial volumes.

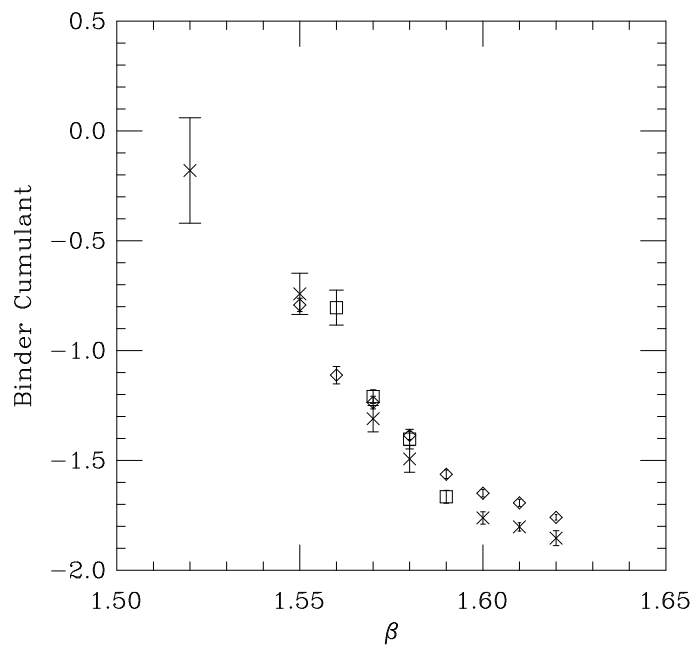


Figure 6: The Binder cumulant for the FP action for $N_t = 4$. Diamond: 8^3 , cross: 10^3 , square: 12^3 spatial volumes.

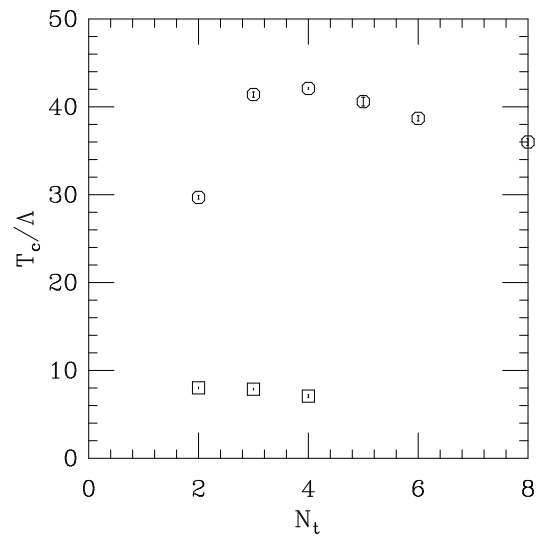


Figure 7: T_c/Λ for the Wilson (octagons) and FP (squares) actions.

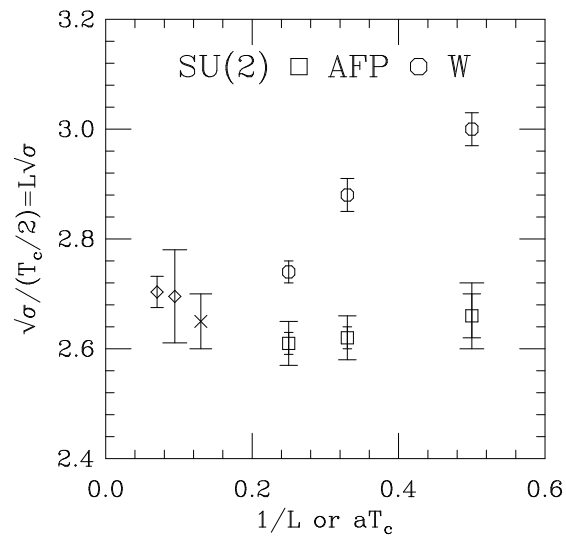


Figure 8: Scaling test of torelon mass on lattices of fixed physical volume for the Wilson action (crosses) and FP action (squares); T_c is defined in infinite spatial volumes. The cross is a torelon mass measurement at $L = 2.07/T_c$ from Ref. 18 and the diamonds are extrapolations by us to $L = 2/T_c$.

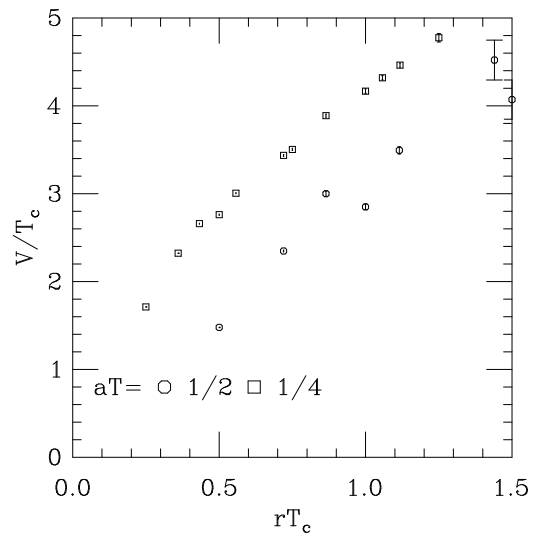


Figure 9: Potential $V(r)/T_c$ vs. rT_c for the Wilson action at $\beta_c(N_T = 2)$ (octagons) and $\beta_c(N_T = 4)$ (squares).

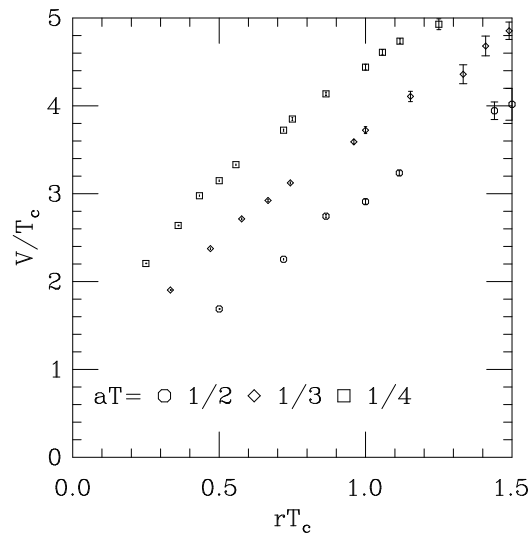


Figure 10: Potential $V(r)/T_c$ vs. rT_c for the FP action at $\beta_c(N_T = 2)$ (octagons), $\beta_c(N_T = 3)$ (diamonds) and $\beta_c(N_T = 4)$ (squares).

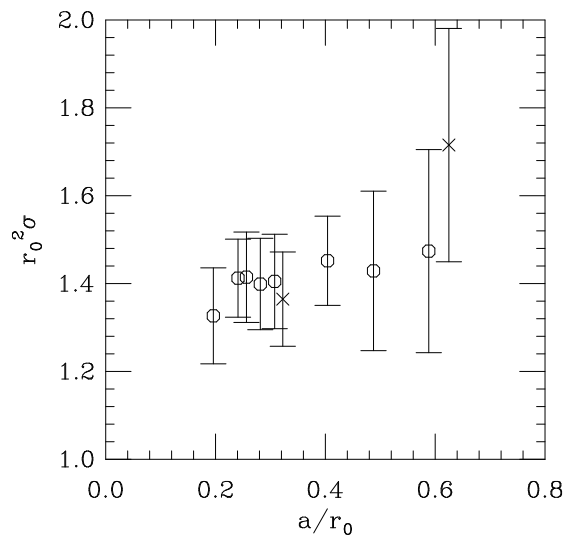


Figure 11: String tension times r_0^2 for the FP action (octagons) and Wilson action (crosses) as a function of r_0/a .

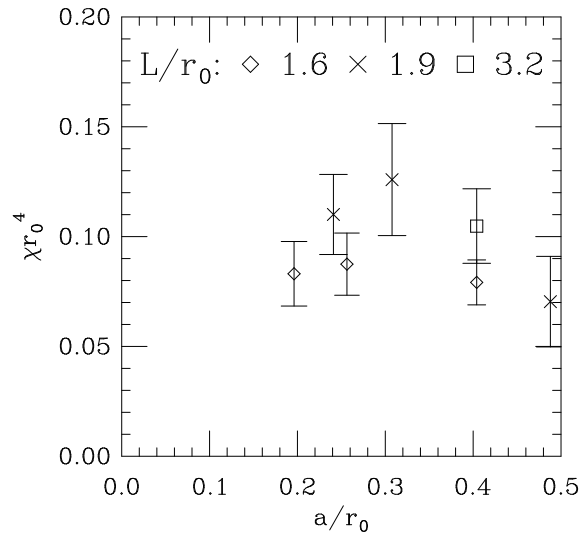


Figure 12: Scaling test for the topological susceptibility, as a function of lattice spacing. The three lattice sizes (in units of r_0) of approximately 1.6, 1.9, and 3.2 are shown by diamonds, crosses, and a square, respectively.